# High Electrical Conductivity in Ni 3 (2,3,6,7,10,11-hexaiminotriphenylene) 2 , a Semiconducting Metal–Organic Graphene Analogue

# High Electrical Conductivity in $Ni_3$(2,3,6,7,10,11-hexaiminotriphenylene)$_2$, a Semiconducting Metal-Organic Graphene Analogue

Dennis Sheberla,[†] Lei Sun,[†] Martin Blood-Forsythe,[‡] Süleyman Er, [‡] Casey R. Wade,[†] Carl K. Brozek,[†] Alán Aspuru-Guzik[‡] and Mircea Dincă*[†]

[†]Department of Chemistry, Massachusetts Institute of Technology, Cambridge, MA, 02139, United States

[‡]Department of Chemistry and Chemical Biology, Harvard University, Cambridge, MA, 02138, United States

*Supporting Information Placeholder*

**ABSTRACT:** Reaction of 2,3,6,7,10,11-hexaaminotriphenylene with $Ni^{2+}$ in aqueous $NH_3$ solution under aerobic conditions produces $Ni_3(HITP)_2$ (HITP = 2,3,6,7,10,11-hexaiminotriphenylene), a new two-dimensional metal-organic framework (MOF). The new material can be isolated as a highly conductive black powder or dark blue-violet films. Two-probe and van der Pauw electrical measurements reveal bulk (pellet) and surface (film) conductivity values of 2 $S \cdot cm^{-1}$ and 40 $S \cdot cm^{-1}$, respectively, both records for MOFs and among the best for any coordination polymer.

Two-dimensional (2D) electronic materials are of considerable interest due to their potential applications in future electronics.[1–3] The most prominent example is graphene, an atomically thin organic 2D material with in-plane π-conjugation.[4] Although graphene exhibits exceptional charge mobility and mechanical stability, its use in semiconductor-based devices is limited by its zero bandgap.[5–7] Dimensional reduction[8] and chemical functionalization[9] can increase the bandgap, rendering graphene semiconducting, but these methods drastically reduce its charge mobility and can introduce numerous defects. This has led to a sustained effort towards identifying 2D materials with intrinsic non-zero bandgaps that could replace conventional semiconductors. Two broad classes of materials have dominated these efforts: the layered metal chalcogenides (e.g. $MoS_2$, $WSe_2$) and 2D covalent-organic frameworks (COFs). The former can be deposited as large-area single sheets in a "top-down" approach.[10,11] They have been shown to perform well in device testing,[12–14] but do not easily lend themselves to chemical functionalization and tunability. In contrast, COFs are prepared by "bottom-up" solution-based synthetic methods and are attractive because they are subject to rational modification.[15,16] Nevertheless, the electronic properties of COFs are largely inferior to metal chalcogenides because the functional groups used to connect their building blocks typically do not allow in-plane conjugation.[17,18]

Bridging the divide between 2D inorganic and organic materials is a recent class of "bottom-up" compounds assembled from multi-topic dithiolene and *o*-semiquinone aromatic organic moieties bridged by square-planar metal ions. These 2D metal-organic networks exhibit non-zero bandgaps and good electrical conductivity enabled by full charge delocalization in the 2D plane.[19–21] They can therefore be described as semiconducting metal-organic graphene analogues (*s*-MOGs). Certain members of this class have also recently been predicted to behave as topological insulators,[22,23] a realm currently dominated by purely inorganic compounds.[24] Clearly, the synthesis and characterization of new *s*-MOGs could give rise to important new electronic materials with exotic electronic states and potential applications in the semiconductor device industry.

Inspired by the success of dithiolene based *s*-MOGs, whose metal linkages mimic classic Class III-delocalized homoleptic Ni(dithiolene)$_2$ complexes,[25,26] we identified Ni(isq)$_2$ (isq = *o*-diiminobenzosemiquinonate) as an attractive target for the construction of a fully charge-delocalized *s*-MOG. Indeed, although first isolated in 1927[27] from *o*-phenylenediamine and $NiCl_2$ in ammoniacal water, Ni(isq)$_2$ evaded structural and electronic characterization for quite a long time,[28,29] but is now known to be fully π-conjugated with its ground state having partial singlet biradical character.[30,31] Crystalline Ni(isq)$_2$ itself exhibits high mobility in organic field effect transistors (OFET)[32] and increased conductivity upon doping with $I_2$.[33] Here, we show that two-dimensional extension of Ni(isq)$_2$ through the reaction of 2,3,6,7,10,11-hexaaminotriphenylene hexahydrochloride (HATP·6HCl) with ammoniacal $NiCl_2$ produces a new crystalline *s*-MOG with very high electrical conductivity, which is linearly proportional to temperature. Remarkably, the conductivity of the new material vastly exceeds those of previous *s*-MOGs and other conductive MOFs and is higher than even some of the best organic conductors.

Under conditions mimicking the synthesis of Ni(isq)$_2$, HATP·6HCl was treated with an aqueous solution of $NiCl_2 \cdot 6H_2O$ under air, followed by the addition of aqueous

$NH_3$ under constant stirring. The reaction mixture was heated to 65 °C and stirred under air for an additional 2 hours. This yielded the new material $Ni_3(HITP)_2$ (HITP = 2,3,6,7,10,11-hexaiminotriphenylenesemiquinonate) as a bulk black powder and a very dark blue-violet film (see Scheme 1). Upon extensive washing with water in an ultrasonic bath, the charge neutrality of $Ni_3(HITP)_2$, and implicitly the formation of monoanionic *o*-diiminobenzosemiquinonate moieties (Scheme 1, bottom), was confirmed by X-ray photoelectron spectroscopy (XPS). As shown in Figure S1 and S2, XPS spectra of both powder and films (vide infra) of $Ni_3(HITP)_2$ show the presence of only Ni, N, C, and O resonance peaks from the material itself and water guest molecules. Cl peaks, expected for any trapped or charge-balancing anionic chlorides that would compensate a possible cationic structure, are absent. Similarly, high-resolution analysis of the Ni(2p) and N(1s) regions of the XPS spectra show a single type of Ni and N atoms, respectively, suggesting that no extraneous $Ni^{2+}$ or $NH_4^+$ ions are present. These ions are the only possible cationic species that could balance an anionic material, and indicate that $Ni_3(HITP)_2$ is indeed neutral, as expected from its similarity with $Ni(isq)_2$.

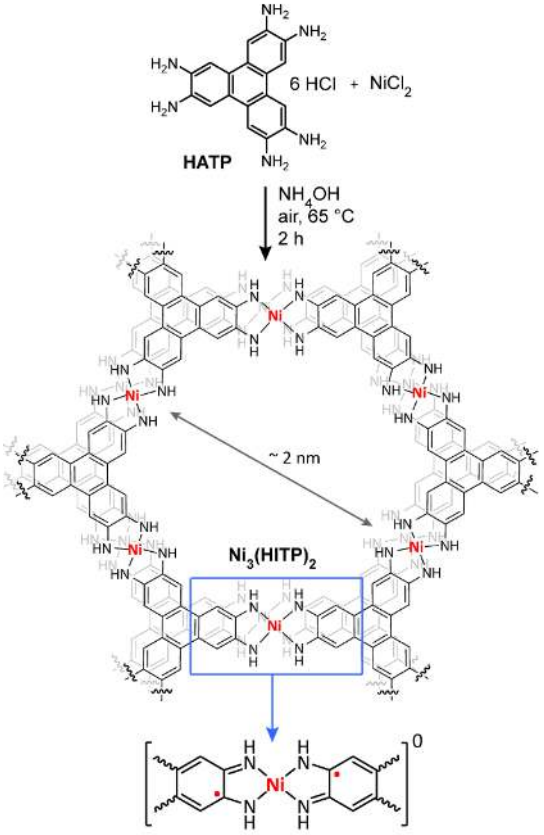


***Scheme 1.*** Synthesis of $Ni_3(HITP)_2$. Only the closed-shell resonance structure is shown, although diradical Ni-bisdiimine linkages, shown on the bottom and found in $Ni(isq)_2$, are likely here too.

Powder X-ray diffraction (PXRD) analysis of $Ni_3(HITP)_2$ revealed a crystalline structure with prominent peaks at $2\theta$ = 4.7°, 9.5°, 12.6°, and 16.5°, indicative of long-range order within the *ab* plane (see Figure 1). An additional, weaker and broader peak at $2\theta$ = 27.3° corresponding to the [001] reflections is indicative of poorer long-rage order along the *c* direction, as expected for covalently-linked layered materials. We simulated several possible stacking arrangements for the 2D sheets of $Ni_3(HITP)_2$, including staggered ($AA^{-1}$), eclipsed (AA), and slipped-parallel (AB) orientations. As shown in Figure 1, the experimental pattern rules out the $AA^{-1}$ stacking, but agrees very well with both the AA and AB sequences. Although the AA and AB sequences are impossible to differentiate on the basis of PXRD alone, Ni K-edge extended X-ray absorption fine structure (EXAFS) analysis of a sample of $Ni_3(HITP)_2$ revealed a spectrum that better agrees with a simulated spectrum of AB than of AA. As shown in Figure S3, a strong Ni···Ni scattering path at $R$ = 3.0 Å (actual Ni···Ni distance = 3.33 Å), expected for AA, is absent in the experimental data.

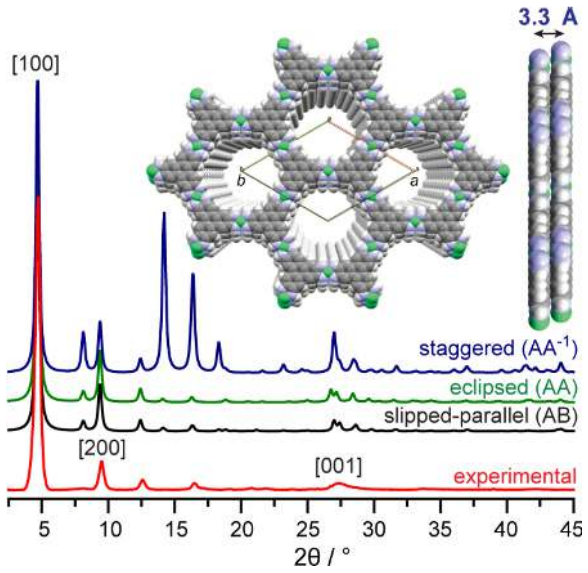


***Figure 1.*** Experimental and simulated PXRD patterns of $Ni_3(HITP)_2$. The inset shows the slipped-parallel structure with neighboring sheets displaced by 1/16 fractional coordinates in the *a* and *b* directions.

Additional support for a slipped-parallel AB stacking model came from DFT calculations (see SI for full details). A model structure was developed by optimizing a hydrogen terminated fragment at the B3LYP-D3BJ/6-31G* level and constraining it to P6/mmm symmetry. A unit cell for the structure was then made by fixing an interlayer separation of 3.3 Å. Periodic single-point energy calculations using the GGA-PBE exchange-correlation functional with D2 dispersion correction were carried out for structures with 82 different *ab*-plane displacements. The potential energy surface shown in Figure 2 was obtained by interpolating DFT total energies using 2D Lagrange polynomials. This potential energy surface suggested that the fully eclipsed AA structure is energetically unfavorable and that the AB sequence is the most stable. In particular, an AB model wherein the 2D unit cell of one layer is slipped relative to a neighboring layer by slightly more than $1/16^{th}$ of a cell edge (~1.8 Å) along the *a* or *b* vectors, gave the lowest energy on the potential energy surface. These calculations do not rule out closely related slipped-parallel structures containing a mixture of displacements to these minima in the potential energy surface, which is consistent with the poorer long-range order along the *c* direction. Altogether, the PXRD, EXAFS, and DFT data evidence a hexagonal $Ni_3(HITP)_2$ structure with slipped-parallel stacking and unit cell parameters $a = b$ = 21.75 Å, and $c$ = 6.66 Å.

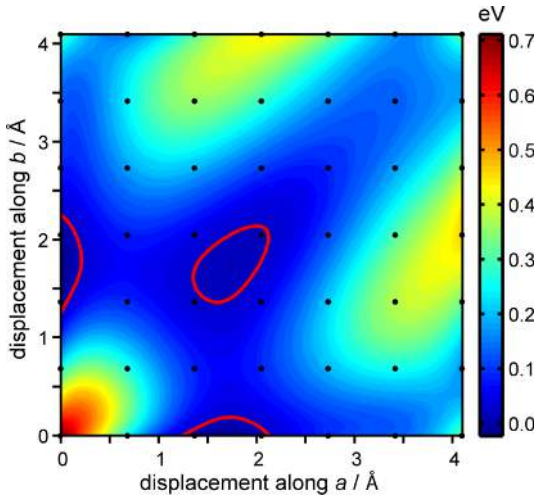


***Figure 2.*** A contour map of the potential energy surface generated by different translations between A and B layers. Black dots correspond to locations of single-point calculations performed using the PBE-D2 functional. Red lines indicate the borders of the 'thermally accessible region' (within $k_BT \approx 0.026$ eV of the minima). The surface was produced by interpolation with 2D Lagrange polynomials on a grid of Chebyshev points. The energy per unit cell has been normalized to zero at the minimum.

With a good structural model in hand, we turned our attention to studying the electronic properties of both bulk and thin films of $Ni_3(HITP)_2$. To allow for optical measurements, we chose quartz as a substrate for our films. Scanning electron microscopy (SEM) and atomic force microscopy (AFM) of representative films of ~500 nm thickness, shown in Figure 3, evidence macroporous surface features and excellent film coverage on the quartz substrate. Importantly, the electronic absorption features of such films extend well into the near-infrared (NIR) range ($\lambda_{max}$ = 1,400 nm), as shown in the UV-Vis-NIR spectrum in Figure S4. Such low energy electronic excitations are common in highly conjugated organics and conducting polymers,[34] but are absent in molecular complexes such as $Ni(isq)_2$, which does not absorb at wavelengths above 900 nm.[29,33]

Encouraged by the possibility of extended 2D conjugation, we measured the electrical properties of $Ni_3(HITP)_2$. To avoid swelling and other solvent effects, we set out to dry our samples for these measurements. A thermogravimetric analysis (TGA) of bulk, freshly cleaned $Ni_3(HITP)_2$, shown in Figure S5, suggested that heating at 150 °C would eliminate all water, and samples used for electrical measurements were dried accordingly.

The first indication of excellent electrical properties in $Ni_3(HITP)_2$ came from a two-probe measurement of bulk powder compressed as a pellet between two stainless steel rods.[35] Despite the small particle size, the numerous intergrain boundaries, and the electrode contact resistances, the pellet conductivity of $Ni_3(HITP)_2$ was 2 S cm$^{-1}$. This is on the same order of magnitude as the two-probe pellet conductivity of some of the best organic conductors,[35] including the iconic TTF-TCNQ ($\sigma_{pellet}$ = 10 S cm$^{-1}$).[36] Furthermore, the bulk conductivity of $Ni_3(HITP)_2$ is one order of magnitude higher than that of the best *s*-MOG (Ni-hexathiobenzene, $\sigma$ = 0.15 S cm$^{-1}$), and at least 2 orders of magnitude better than the most conducting MOFs to date.[37–39]

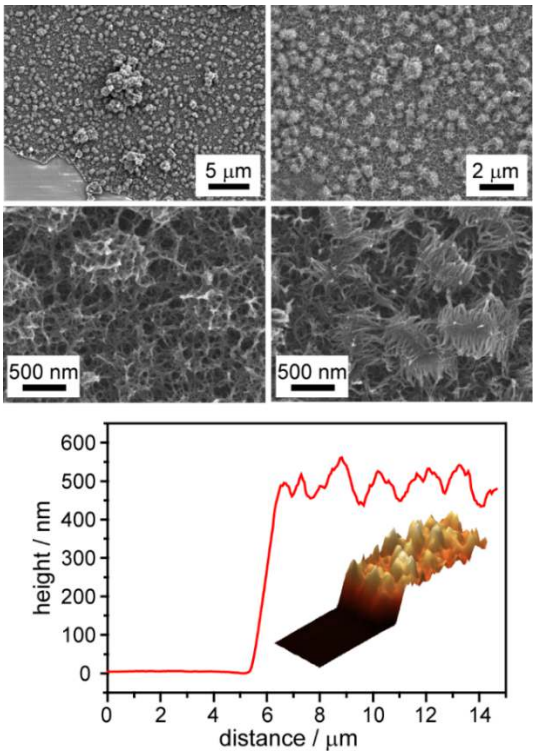


***Figure 3.*** Top: SEMs for films of $Ni_3(HITP)_2$ at various magnifications. Bottom: AFM thickness profile and corresponding 3D AFM image of a representative $Ni_3(HITP)_2$ film.

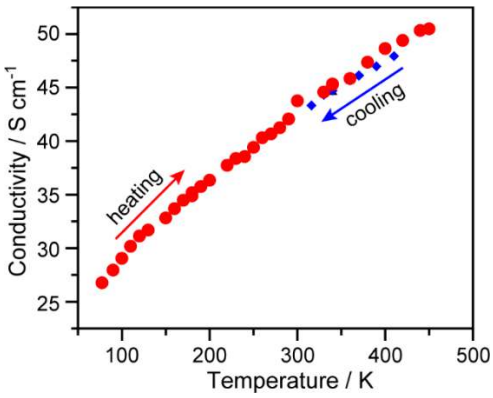


***Figure 4.*** Variable temperature van der Pauw conductivity measurement on a ~500 nm thick film on quartz.

Even more remarkable results were obtained for thin films, configurations that are likely more relevant for future devices. Thus, films of $Ni_3(HITP)_2$ deposited on quartz substrates consistently gave conductivity values of 40 S cm$^{-1}$ at room temperature, as measured by the van der Pauw method.[40] The conductivity showed linear increase with temperature from 77 K to 450 K, as shown in Figure 4, a behavior that was reversible upon cooling. Although we have been unable to find a model that unequivocally explains this behavior over the entire temperature range, organic-based semiconductors are notorious for having complicated, mixed charge transport mechanisms;[41–43] further theoretical and experimental studies will probe the mechanism that is operative here. Most notably, among all coordination

polymers,[44] the film conductivity of $Ni_3(HITP)_2$ is exceeded only by Cu(4-hydroxythiophenolate) ($\sigma$ = 120 S·cm$^{-1}$).[45]

Clearly, the nature of charge transport in $Ni_3(HITP)_2$ and its undoubtedly superior single sheet electrical properties warrant further studies, as do its magnetic behavior and its inclusion in electronic devices. The more general picture afforded by these studies, nevertheless, is that metals can mediate very efficient 2D conjugation pathways between electroactive organic molecules, leading to new materials with impressive electrical properties. Although this could perhaps be already gleaned from the vast literature on molecular conductors, the successful application of these concepts to two- and three-dimensionally extended crystalline networks is just emerging and promises to take us on a thrilling intellectual ride.

## ASSOCIATED CONTENT

### Supporting Information

Experimental details, EXAFS, XPS, TGA, UV-Vis plots, and additional AFM images. This material is available free of charge via the Internet at http://pubs.acs.org.

## AUTHOR INFORMATION


### Corresponding Author

mdinca@mit.edu


## ACKNOWLEDGMENT


Synthetic work was supported by the U.S. Department of Energy, Office of Science, Office of Basic Energy Sciences (U.S. DOE-BES), under Award DE-SC0006937. Physical measurements were supported as part of the Center for Excitonics, an Energy Frontier Research Center funded by the U.S. DOE-BES under award no. DE-SC0001088 (MIT). M.D. gratefully acknowledges early career support from the Sloan Foundation, the Research Corporation for Science Advancement (Cottrell Scholar), and 3M. C.K.B. is partially supported by an NSF Graduate Research Fellowship through Grant 1122374. M.B.F. acknowledges support by the U.S. DOE, Graduate Fellowship Program, administered by ORISE-ORAU under contract no. DE-AC05-06OR23100. S.E. performed work as part of the Fellowships for Young Energy Scientists program of the Foundation for Fundamental Research on Matter (FOM), which is part of the Netherlands Organization for Scientific Research (NWO). A.A-G. acknowledges support from the NSF Center for Integrated Quantum Materials (CIQM) through grant NSF-DMR-1231319. Computational research was carried out in part at the Center for Functional Nanomaterials, which is supported by the U.S. DOE under Contract No. DE-AC02-98CH10886. We also thank Dr. Jeffrey Miller for assistance with the collection of X-ray absorption data at the Advanced Photon Source, beamline 10-BM, which is operated for the U.S. DOE by Argonne National Laboratory, and supported under Contract No. DE-AC02-06CH11357.


## REFERENCES


(1) Weiss, N. O.; Zhou, H.; Liao, L.; Liu, Y.; Jiang, S.; Huang, Y.; Duan, X. *Adv. Mater.* **2012**, *24*, 5782–5825.

(2) Xu, M.; Liang, T.; Shi, M.; Chen, H. *Chem. Rev.* **2013**, *113*, 3766–3798.

(3) Butler, S. Z. et al. *ACS Nano* **2013**, *7*, 2898–2926.

(4) Novoselov, K. S.; Geim, A. K.; Morozov, S. V; Jiang, D.; Zhang, Y.; Dubonos, S. V; Grigorieva, I. V; Firsov, A. A. *Science* **2004**, *306*, 666–669.

(5) Novoselov, K. S.; Geim, A. K.; Morozov, S. V; Jiang, D.; Katsnelson, M. I.; Grigorieva, I. V; Dubonos, S. V; Firsov, A. A. *Nature* **2005**, *438*, 197–200.

(6) Castro Neto, A. H.; Guinea, F.; Peres, N. M. R.; Novoselov, K. S.; Geim, A. K. *Rev. Mod. Phys.* **2009**, *81*, 109–162.

(7) Avouris, P. *Nano Lett.* **2010**, *10*, 4285–4294.

(8) Ruffieux, P.; Cai, J.; Plumb, N. C.; Patthey, L.; Prezzi, D.; Ferretti, A.; Molinari, E.; Feng, X.; Müllen, K.; Pignedoli, C. A.; Fasel, R. *ACS Nano* **2012**, *6*, 6930–6935.

(9) Georgakilas, V.; Otyepka, M.; Bourlinos, A. B.; Chandra, V.; Kim, N.; Kemp, K. C.; Hobza, P.; Zboril, R.; Kim, K. S. *Chem. Rev.* **2012**, *112*, 6156–6214.

(10) Mak, K. F.; Lee, C.; Hone, J.; Shan, J.; Heinz, T. F. *Phys. Rev. Lett.* **2010**, *105*, 136805.

(11) Chhowalla, M.; Shin, H. S.; Eda, G.; Li, L.-J.; Loh, K. P.; Zhang, H. *Nat. Chem.* **2013**, *5*, 263–275.

(12) Radisavljevic, B.; Radenovic, A.; Brivio, J.; Giacometti, V.; Kis, A. *Nat. Nanotechnol.* **2011**, *6*, 147–150.

(13) Baugher, B. W. H.; Churchill, H. O. H.; Yang, Y.; Jarillo-Herrero, P. *Nat. Nanotechnol.* **2014**, *in press*.

(14) Wang, Q. H.; Kalantar-Zadeh, K.; Kis, A.; Coleman, J. N.; Strano, M. S. *Nat. Nanotechnol.* **2012**, *7*, 699–712.

(15) Gutzler, R.; Perepichka, D. F. *J. Am. Chem. Soc.* **2013**, *135*, 16585–16594.

(16) Colson, J. W.; Dichtel, W. R. *Nat Chem* **2013**, *5*, 453–465.

(17) Bertrand, G. H. V; Michaelis, V. K.; Ong, T.-C.; Griffin, R. G.; Dincă, M. *Proc. Natl. Acad. Sci.* **2013**, *110*, 4923–4928.

(18) An example of a COF exhibiting full in-plane conjugation has been reported recently: Guo, J.; Xu, Y.; Jin, S.; Chen, L.; Kaji, T.; Honsho, Y.; Addicoat, M. a; Kim, J.; Saeki, A.; Ihee, H.; Seki, S.; Irle, S.; Hiramoto, M.; Gao, J.; Jiang, D. *Nat. Commun.* **2013**, *4*, 2736.

(19) Hmadeh, M.; Lu, Z.; Liu, Z.; Gándara, F.; Furukawa, H.; Wan, S.; Augustyn, V.; Chang, R.; Liao, L.; Zhou, F.; Perre, E.; Ozolins, V.; Suenaga, K.; Duan, X.; Dunn, B.; Yamamto, Y.; Terasaki, O.; Yaghi, O. M. *Chem. Mater.* **2012**, *24*, 3511–3513.

(20) Kambe, T.; Sakamoto, R.; Hoshiko, K.; Takada, K.; Miyachi, M.; Ryu, J.-H.; Sasaki, S.; Kim, J.; Nakazato, K.; Takata, M.; Nishihara, H. *J. Am. Chem. Soc.* **2013**, *135*, 2462–2465.

(21) Cui, J.; Xu, Z. *Chem. Commun.* **2014**, in press.

(22) Wang, Z. F.; Liu, Z.; Liu, F. *Nat. Commun.* **2013**, *4*, 1471.

(23) Wang, Z. F.; Su, N.; Liu, F. *Nano Lett.* **2013**, *13*, 2842–2845.

(24) Kong, D.; Cui, Y. *Nat. Chem.* **2011**, *3*, 845–849.

(25) Sproules, S.; Wieghardt, K. *Coord. Chem. Rev.* **2011**, *255*, 837.

(26) Eisenberg, R.; Gray, H. B. *Inorg. Chem.* **2011**, *50*, 9741–9751.

(27) Feigl, F.; Fürth, M. *Monatsh. Chem.* **1927**, *48*, 445–450.

(28) Stiefel, E. I.; Waters, J. H.; Billig, E.; Gray, H. B. *J. Am. Chem. Soc.* **1965**, *87*, 3016–3017.

(29) Herebian, D.; Bothe, E.; Neese, F.; Weyhermüller, T.; Wieghardt, K. *J. Am. Chem. Soc.* **2003**, *125*, 9116–9128.

(30) Bachler, V.; Olbrich, G.; Neese, F.; Wieghardt, K. *Inorg. Chem.* **2002**, *41*, 4179–4193.

(31) Fukui, H.; Shigeta, Y.; Nakano, M.; Kubo, T.; Kamada, K.; Ohta, K.; Champagne, B.; Botek, E. *J. Phys. Chem. A* **2011**, *115*, 1117–1124.

(32) Noro, S.; Chang, H.-C.; Takenobu, T.; Murayama, Y.; Kanbara, T.; Aoyama, T.; Sassa, T.; Wada, T.; Tanaka, D.; Kitagawa, S.; Iwasa, Y.; Akutagawa, T.; Nakamura, T. *J. Am. Chem. Soc.* **2005**, *127*, 10012–10013.

(33) Lelj, F.; Morelli, G.; Ricciardi, G.; Brigatti, M. F.; Rosa, A. *Polyhedron* **1989**, *8*, 2603–2610.

(34) Skotheim, T. A.; Reynolds, J. R., Eds. *Handbook of conducting polymers*; 3rd ed.; CRC Press: Boca Raton, FL, 2007.

(35) Wudl, F.; Bryce, M. R. *J. Chem. Educ.* **1990**, *67*, 717.

(36) Wheland, R. C.; Gillson, J. L. *J. Am. Chem. Soc.* **1976**, *98*, 3916–3925.

(37) Gándara, F.; Uribe-Romo, F. J.; Britt, D. K.; Furukawa, H.; Lei, L.; Cheng, R.; Duan, X.; O'Keeffe, M.; Yaghi, O. M. *Chem. – A Eur. J.* **2012**, *18*, 10595–10601.

(38) Kobayashi, Y.; Jacobs, B.; Allendorf, M. D.; Long, J. R. *Chem. Mater.* **2010**, *22*, 4120–4122.
(39) Talin, A. A.; Centrone, A.; Ford, A. C.; Foster, M. E.; Stavila, V.; Haney, P.; Kinney, R. A.; Szalai, V.; El Gabaly, F.; Yoon, H. P.; Léonard, F.; Allendorf, M. D. *Science* **2013**.
(40) Van der Pauw, L. J. *Philips Tech. Rev.* **1958**, *20*, 220–224.
(41) Menon, R.; Yoon, C. O.; Moses, D.; Heeger, A. J. In *Handbook of conducting polymers*; Skotheim, T. A.; Elsenbaumer, R. L.; Reynolds, J. R., Eds.; Marcel Dekker: USA, 1998.
(42) Coropceanu, V.; Cornil, J.; da Silva Filho, D. A.; Olivier, Y.; Silbey, R.; Brédas, J.-L. *Chem. Rev.* **2007**, *107*, 926–952.
(43) Baranovski, S., Ed. *Charge Transport in Disordered Solids with Applications in Electronics*; Wiley: New York, 2006.
(44) Givaja, G.; Amo-Ochoa, P.; Gomez-Garcia, C. J.; Zamora, F. *Chem. Soc. Rev.* **2012**, *41*, 115–147.
(45) Low, K.-H.; Roy, V. A. L.; Chui, S. S.-Y.; Chan, S. L.-F.; Che, C.-M. *Chem. Commun.* **2010**, *46*, 7328–7330.

TOC graphic